17th World Conference on Earthquake Engineering, 17WCEE
Sendai, Japan - September 13th to 18th 2020

CUMULATIVE DAMAGE IN RC BUILDINGS – THE CASE OF THE 2017 PUEBLA-MORELOS EARTHQUAKE

L. Massone[(1)], D. Aceituno[(2)], J. Carrillo[(3)]

[(1)] *Associate Professor, University of Chile, lmassone@uchile.cl*
[(2)] *Ms Student, University of Chile, diego.aceituno@ing.uchile.cl*
[(3)] *Associate Professor, Nueva Granada Military University, julian.carrillo@unimilitar.edu.co*

Abstract

The dynamic nature of earthquakes causes cyclic loading in structures. This seismic loading imposes tensile/compressive cyclic strain demands in reinforcement of columns, walls and other structural elements. When the demand is high enough, the structure can endeavor once or several times into plastic response causing permanent damage. Depending on the number of cycles and the strain levels achieved in each cycle, cumulative damage can lead to fatigue of steel reinforcement in reinforced concrete (RC) structures. Although the concept of cumulative damage caused by earthquakes is widely known, current design codes commonly fail in considering such effects for successive or long-duration seismic events. The Puebla-Morelos Earthquake (Mw7.1) occurred in Mexico on 19 September 2017 leaving 44 buildings collapsed in Mexico City of which 91% were built before 1985. It is very attractive to study cumulative damage during this earthquake, since most of the collapsed buildings correspond to old structures that previously supported the devastating earthquake occurred in Michoacán (Mw8.1) on 19 September 1985. The hypothesis of this investigation is that the buildings collapsed due to the plastic damage accumulated during both events and not by the level of seismic demand of the last earthquake, as it is usually thought. It is assessed in this study the performance of structures that have been subjected to more than one considerable seismic event since its construction, incorporating the accumulated damage through low-cycling fatigue models. The methodology of this work is based on evaluating the non-linear response of a prototype model (characteristic of Mexican pre-1985 structures) that is subjected to seismic excitations recorded during the earthquakes of 1985 and 2017 in different places in Mexico City. The building response is assessed through a damage index (DI) that considers cycles with different peak values of axial strain of steel reinforcement and local plastic damage accumulated by the structure during both seismic events. The calculated ID is mapped not only for visualizing the areas of the city where buildings were damaged or collapsed, but also for comparing with areas where damage was not observed.

Keywords: Puebla-Morelos earthquake; cumulative damage; low-cycle fatigue; damage index, reinforced concrete buildings.

1. Introduction

Most existing studies to date focus on generating global damage spectra from simplified systems of 1 degree of freedom (SDOF). These are calculated from the maximum ductility and/or the internal energy dissipated by the system during the seismic action. The most recognized damage index is the one by Park and Ang [1] that combines both components; however, some authors suggest that energy-based models can lead to better approximations of accumulated damage [2-6]. In this way, a relevant approach to incorporate low-cycle fatigue was made by Cao *et al*. [2] and Chai [3], who also related, in terms of energy, the monotonic capacity with the number of constant amplitude cycles that the structure is able to undergo before failure. On the other hand, based on displacement spectra and damage observed in past earthquakes, Rodríguez [5] proposed an energy-based index that considers the type and the stiffness of the structural system at issue.

Although the intention of all these simplified models is to consider fatigue damage, none is able to relate the cyclic deformation of the material with its respective capacity through a consistent material constitutive law. That means that they do not necessarily distinguish between local failure modes, such as concrete crushing or bar buckling. Moreover, even though there is vast information on progressive damage models, most current code-based designs procedures and analyses of structures do not consider cumulative damage that could affect the response of buildings subjected to more than one earthquake.

The structural system of prototype model considered in this study was the most common structural system with damage reported in Mexico City after the 2017 Puebla-Morelos Earthquake. Seismic records of the 2017 Puebla-Morelos (Mw7.1) and 1985 Michoacán (Mw8.1) earthquakes are assessed in order to understand the impact of accumulated damage on parameters such as displacement spectra, given that most damaged structures were subjected to both earthquakes with similar demands. The inelastic response of the archetype building will be assessed with the objective to relate low-cycle fatigue of steel as cause of collapse in different places of the city.

2. The Puebla-Morelos 2017 Mexico Earthquake

A brigade of Civil Engineers of Mexico (CICM) inspected a total of 1997 buildings that showed some type of visible damage and rated 460 of them (23%) as high-risk structures due to the presence of significant structural damage, differential settlements or severe non-structural damage [7]. This damage was concentrated in a specific area of the city that extends along the soils types II, IIIa and IIIb, of the seismic zoning incorporated on 2004 (Fig. 2a), which is characterized by high levels of seismic amplification due to the presence of soft clay layers with thickness between 20 and 45 m [8]. In fact, geotechnical characterization identified a high level of resonance in these soil types, causing high spectral accelerations for structural periods between 0.8-1.6 seconds and generating significant damage in many structures between 5 and 8 stories high [9].

Many researchers [10-13] have indicated that most of the damaged buildings were built before 1985 and were characterized with a soft first story based on a flat slab system supported by RC columns. In first place, soft first story provides stiffness and lateral resistance much lower than the upper floors, given that buildings were commonly designed with large parking spaces and the upper floors with brick masonry infill walls (Fig. 1). Also, the flat slab system supported by RC columns provides limited ductility, especially in structures designed prior to 1985 with poor code-based detailing requirements. The combination of these elements triggers that lateral deformations concentrates in the first floor during the earthquake, which also leads to local failures of columns having inadequate details and spacing of stirrups. When a column loses its resistant capacity, the loads are suddenly transferred to the adjacent columns generating a subsequent fragile failure and a failure path effect that leads to total collapse [8].

Galvis *et al*. [8] state the importance of considering cumulative earthquake damage and indicate that the degradation of lateral stiffness in non-ductile RC structures may have played an important role in the performance of structures that collapsed during the 2017 Puebla-Morelos earthquake. Moreover, the number of collapsed masonry structures (both confined and unreinforced) contributes 6% of the collapses documented in 1985 versus 33% observed in 2017; this trend evidences effects of accumulated damage in the performance

of this type of structures, considering that the spectral ordinates of both earthquakes were similar in the range of periods of the damaged structures [14].

Fig. 1 – (a) Building with soft floor [15] and collapse [16], (b) Prototype building [17].

2.1 Seismic Stations of Mexico City in 2017

A collection of seismic records was obtained from the Center for Instrumentation and Seismic Records (CIRES), the Accelerographic Network of the Institute of Engineering (RAII), and the Seismic Network of the Valley of Mexico (RSVM). The map showed in Fig. 2b was constructed using this information; this map shows the coverage of seismic stations in Mexico City during the 2017 earthquake. There are 58 CIRES records, 6 RAII records and 8 RSVM records delivering a total of 72 seismic records available and uniformly distributed in the urban area of the city. The data provided in this study were processed including the correction of the baseline, and the filtering of high and low frequencies with a low pass filter of 8th order with 0.1Hz and a high pass filter of 4th order with 30Hz, respectively, both of the Butterworth type.

2.2 Collapsed Buildings

An extent of 44 buildings between 1 and 11 stories high were considered collapsed over a vast area of the city [16] (Fig. 2a). Fig. 2a shows that the damage was concentrated in a fairly narrow strip that extends 18 km in the NS direction of the west side of Mexico City, although it is also observed 4 collapses outside this area that may be related to local soil effects or other factors.

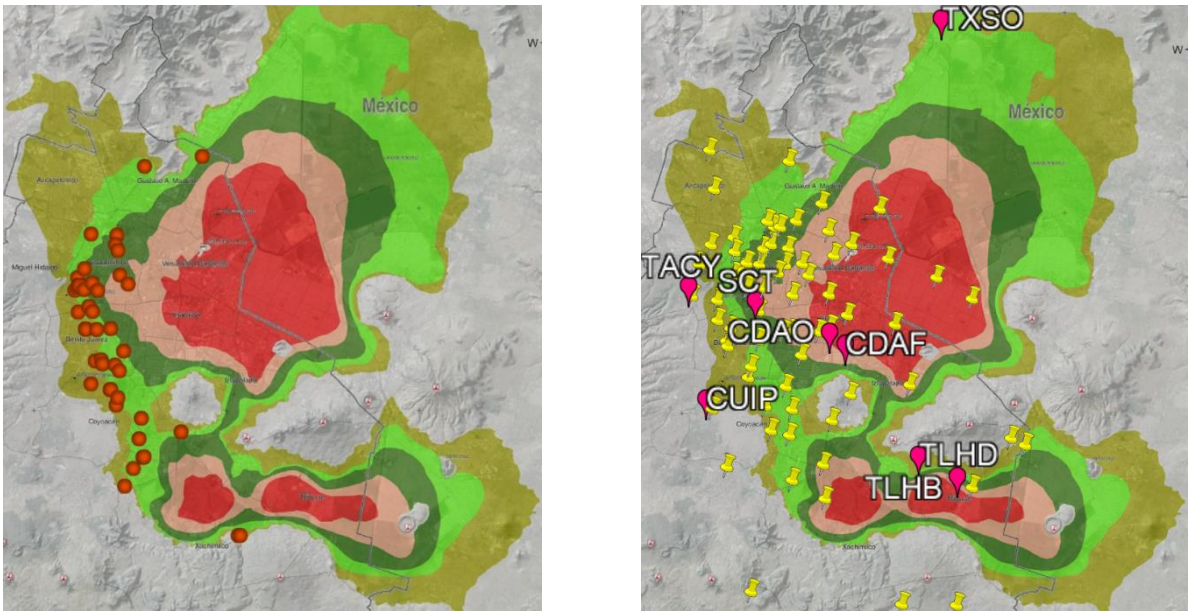

Fig. 2 – (a) Location of 44 collapsed buildings, (b) Seismic records for the study.

2.3 Prototype Building

Although the code that governs the design of buildings in Mexico City has been in a continuous process of updating, there are still many flexible structures built before 1985 that have low ductility capacity and were extremely damaged during the Puebla-Morelos earthquake in 2017. With the objective of explain the damage observed in these types of structures, Arteta *et al*. [17] studied two sets of 6-story buildings based on RC moment frames each with different configurations of masonry infill walls (frames with totally or partially filled masonry walls). The first set of buildings was designed for low ductility (design strength reduction factor Q = 2) and the second was designed for medium ductility (Q = 4), according to all the requirements prescribed in the Mexico City Building Standards for Seismic Design and for Concrete Structures (NTC-C and NTC-S) of 1976 which regulated the structural design from 1976 to 1987 in Mexico City. The main difference between both sets is the implementation of special detailing provisions for Q = 4 according to section 4.7 of the NTC-C (1976), while the seismic coefficient used for the equivalent static method of all models was c=0.24 because most of the collapsed structures were built on soft soils according to the zoning of the NTC-S [17].

In this study, date of construction of the collapsed buildings was investigated observing that most of them were actually built between the 60's and 70's, i.e., they were designed according to older design requirements than those prescribed in NTC of 1976. A review of the Construction Regulations for Federal District (RCFD) of 1942 and 1962 were carried out. However, it is considered that regularized design of structures in terms of required strength for RC flexible frames with partially filled masonry walls and designed with Q=2 is a well-representative model of the pre-1985 damaged structures. This given that strength requirements for pre-1976 design code are closer to a design code level for Q~4 in the NTC of 1976, that accompanied with an estimated overstrength of Ω=2 would yield a structure design for Q=2 with actual material properties.

3. Dynamic Analysis and Cumulative Damage

For the nonlinear dynamic analyses, mass and stiffness-proportional Rayleigh damping was included to simulate the energy dissipation characteristics of the building not represented by the nonlinear behavior of the framing elements. The coefficients in the Rayleigh damping formulation were established to achieve a damping ratio of ζ=5% at the first vibrational period of the model. The initial period of vibration (T_0) after applying the gravitational loading is 0.74 seconds in the main direction. Period of vibration associated to cracked cross-sections is estimated at 1.3 seconds.

On the other hand, the fact that not all stations of 2017 have recorded the 1985 earthquake is a limitation in this investigation. In order to study this phenomenon and make reasonable assumptions of station selection where seismic records of the 1985 earthquake are not available, spectral analysis of seismic demands registered by all 1985 operative stations is done in this study.

3.1 Ground Motions of 1985 Earthquake

There are 8 available seismic records of the 1985 earthquake in Mexico City (Fig. 2b - 1985 in pink and labeled; 2017 in yellow). Two of them were located on rock or firm soil (CUP5 and TACY), one on soil IIIa (TXSO), three on soil IIIb (CDAF, SCT and TLHD), one on soil IIIc (CDAO) and one on soil IIId (TLHB), while there are no seismic records on soil II.

For those records on soft soil, a comparison between their seismic demands in terms of maximum inelastic displacement (Sdi) and dissipated plastic energy (Eh) spectra is carried out for the periods ranging from 0.5 to 3.0 seconds. For simplicity, a SDOF oscillator was used. In order to select the resistance of the prototype building with representability, the yield strength was defined as same as indicates the 1976 design spectrum for Q=2 in soft soil. As an approximation, an elastic-perfectly plastic material law was used. Critical damping of 5% was defined, as it is commonly defined in code-based design. The solution method was the one specified by Newmark-Halls [18] with the linear acceleration assumption, γ=1/2 and β=1/6. Energy spectra were normalized by the mass of the system.

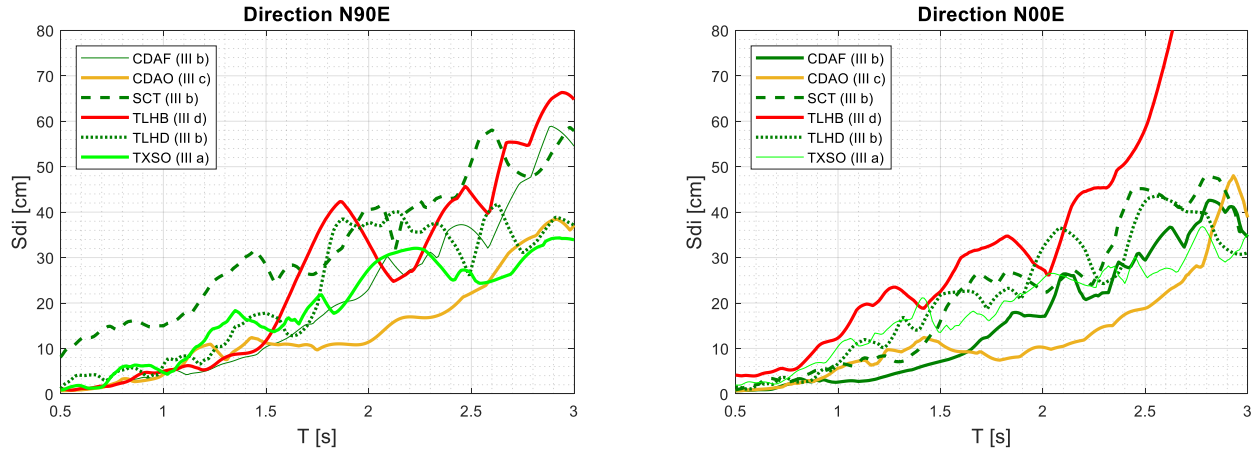

Fig. 3 – Maximum inelastic displacement spectra of 1985 seismic records in both directions.

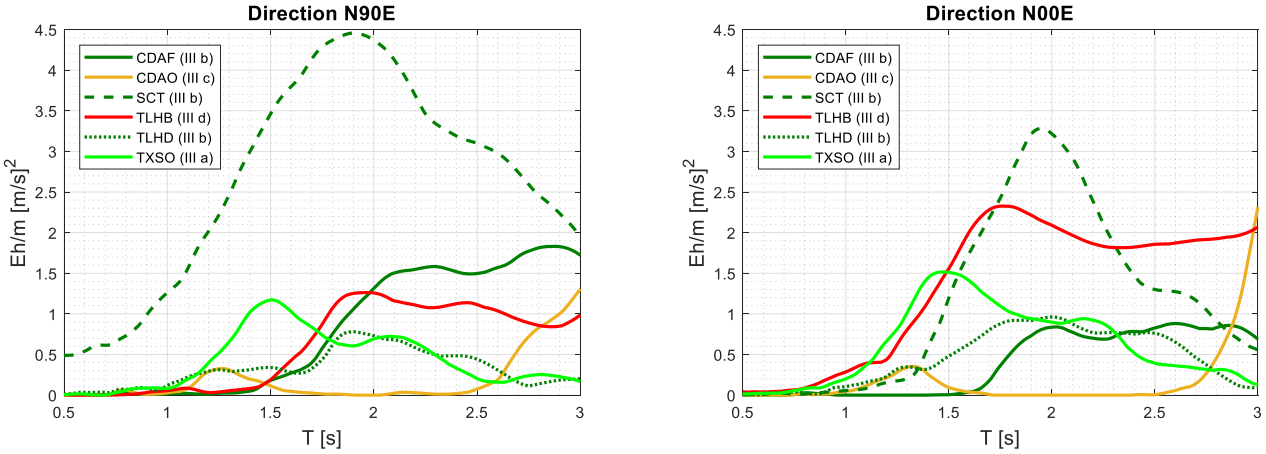

Fig. 4 – Normalized Eh spectra of 1985 seismic records in both directions.

Assuming that the whole structure is modeled as a SDOF system whose properties are capable of simulating global behavior in the range of period of interest from 0.8 to 1.5 seconds, the maximum inelastic displacement of all records are not greater than 20 cm, except for the SCT record that reaches 31.5 cm in the N90E direction (Fig 3). In the same way, the plastic energy dissipation is markedly higher for the SCT record in the N90E direction, although in the N00E direction the demand is slightly greater for TLHB and TXSO stations (Fig 4). These results are consistent with the expected soil resonance of soil type IIIa, IIIb and non-resonance of soil type IIId and rock, while TLHB demand on soil IIId exhibited important amplification as well.

For this study, one station per seismic zone will be used as a representative station/record of the 1985 earthquake since there is a lot more data available in 2017 and soil effects should not be neglected. For rock, CUIP station is selected, while for soil type II and IIIb SCT station is selected since some amplification is expected. Soil types IIIa and IIId will be characterized with its only available seismic record.

3.2 Theoretical Framework

Seismic loading on structures impose tensile/compressive cyclic strain demands in reinforcement of columns, walls or other structural elements. When the demand is high enough, the structure can endeavor once or several times into plastic response causing permanent damage. The accumulation of low-cycle fatigue damage can lead to a premature failure of reinforcing bar in a relatively smaller number of cycles. In RC structures designed to predominantly respond in a flexure mode during a seismic event, their ultimate failure is primarily associated

with either fracture of reinforcing bars due to accumulation of low-cycle fatigue damage, or buckling of reinforcing bars due to inadequate lateral restraint provided by the transverse reinforcement, or crushing of core concrete due to inadequate confinement reinforcement [19].

A simple method to predict fatigue life of reinforcing bars with reasonable accuracy was presented by Tripathi *et al*. [19]. The proposed model allows estimating the cyclic capacity of reinforcing bars in terms of the number of half cycles needed to reach failure at certain level of total strain amplitude. In that study, the buckling of a reinforcing bar is known to depend on its yield strength (fy) and slenderness ratio (L/D), and its behavior can be defined by using a nondimensional buckling parameter (λ) that is computed using Eq. (1).

$$\lambda = \frac{L}{D}\sqrt{\frac{fy}{100}} \tag{1}$$

where the slenderness ratio (L/D) is the ratio of the unsupported length (i.e. buckling length, L) to diameter (D) of the bar. Observations suggest that increase in slenderness ratio of the reinforcing bars results in substantial reduction of their low-cycle fatigue life [14]. In the case of collapsed buildings in Mexico City, slenderness ratio L/D~20 was commonly observed. Therefore, the low-cycle fatigue life of reinforcing bars can be evaluated using total strain amplitude (ε_a) given by the Eq. (2).

$$\varepsilon_a = \beta(2Nf)^a \tag{2}$$

where 'β' is the fatigue ductility coefficient and 'a' is the fatigue ductility exponent, which can be calibrated using experimental test results, and 'Nf' is the number of cycles to the onset of failure. Low-cycle fatigue life of Grade 300E and 500E reinforcing bars was evaluated by testing on un-machined specimens subjected to constant axial strain loading with amplitude ranging from 1% to 5 and different slenderness ratios. The calibration resulted on the Eqs. (3) and (4) for ductility fatigue exponent and coefficient respectively [19]. Thus, strength of steel was defined as fy=483 MPa on prototype model so corresponding cycle life of reinforcing bars considering the low-cycle failure model can be constructed (Fig. 5) with Eqs. (1-4).

$$a = -\left(\frac{\lambda}{1200} + 0.441\right) \tag{3}$$

$$\beta = \frac{-\lambda}{350} + 0.2 \tag{4}$$

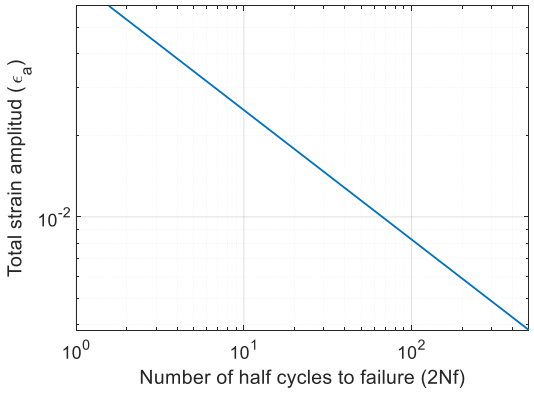

Fig. 5 – Low cycle fatigue life of reinforcing bars.

3.3 Methodology

The expected behavior of the case-study building is assessed by inelastic analyses considering static and dynamic loading effects. The computational software *OpenSees* [20] is selected for this purpose. As mentioned before, there are 72 seismic records available and uniformly distributed over Mexico City. Both directions

N90E and N00E are evaluated independently so that a total of 144 dynamic analyses were performed. Each one considers a single seismic record of 1985, followed by a single seismic record of 2017.

Main results from dynamic response of prototype building subjected to SCT records in the N90E direction are shown in this section in order to explain the methodology to calculate damage index considering the low-cycle fatigue life model of reinforcing bars. The first step is to obtain the cyclic strain-stress response of reinforcing bar (modeled as fibers, Fig. 6) for columns at first floor since larger cyclic demands are concentrated there in comparison with the upper floor columns. Fig. 6 shows the extreme fibers (reinforcing bars) behavior of the bottom central column. Fig. 7 shows the strain-time history for the values obtained for the bottom central column. The first 240 seconds of the recording correspond to 1985 earthquake, followed by the 2017 earthquake.

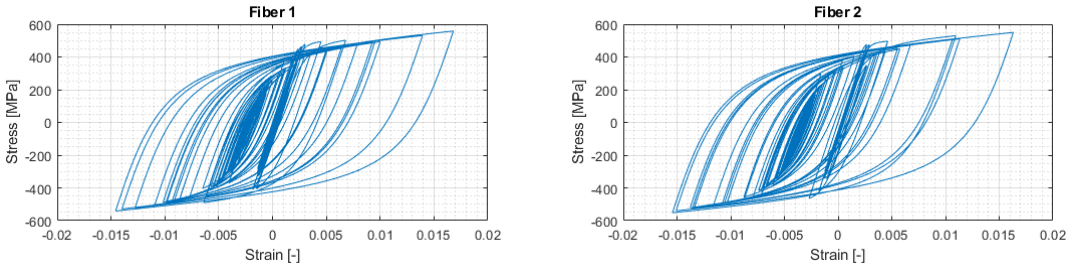

Fig. 6 –Cyclic stress-strain response of reinforced bars for SCT 1985 plus 2017 seismic records of central bottom column.

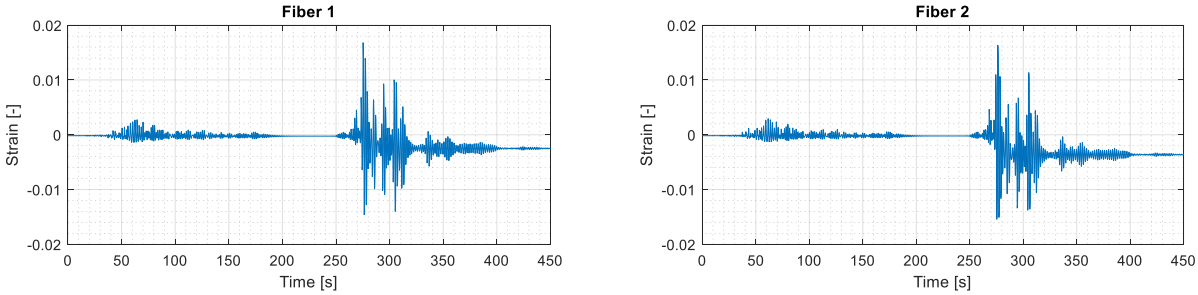

Fig. 7 – Cyclic strain time history of extreme fibers (reinforcing bars) of bottom central column.

In the first portion of record, reinforcing bars hardly reached yield strain, but then a maximum 0.017 strain value is reached. Residual strain of 0.004 can be observed in compression. In order to calculate the total strain amplitude of each half cycle, peak strains must be identified. Every absolute difference between one peak and an adjacent one is named $\Delta\varepsilon_a$ or total strain (Fig. 8) corresponding to a half cycle (2Nf), in order to make a rain flow counting possible [21].

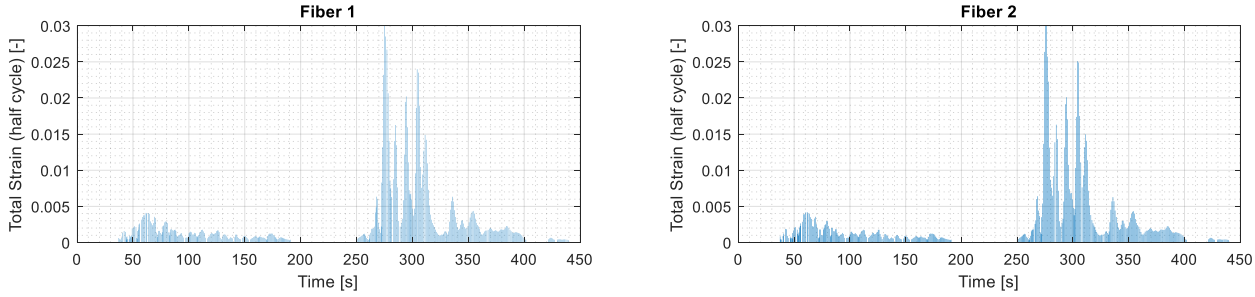

Fig 8 – Total strain ($\Delta\varepsilon_a$) for each half cycle (2Nf) of bottom central column.

The low-cycle fatigue life model of Tripathi *et al*. [19] is introduced to count damage from each half cycle (D_i). This quantity is defined in Eq. (5), following Eqs. (1-4) that define the cyclic capacity of reinforcing bars.

The absolute damage index (DI) is calculated as the sum of all terms using Eq. (6). With those considerations, progression of accumulated damage in time can be also plotted in Fig. 9.

$$D_i = \left(\frac{1}{2Nf}\right)_i = \left(\frac{\Delta\varepsilon_a}{\beta}\right)_i^{1/a} \tag{5}$$

$$DI = \sum_i D_i = \sum_i \left(\frac{\Delta\varepsilon_a}{\beta}\right)_i^{1/a} \tag{6}$$

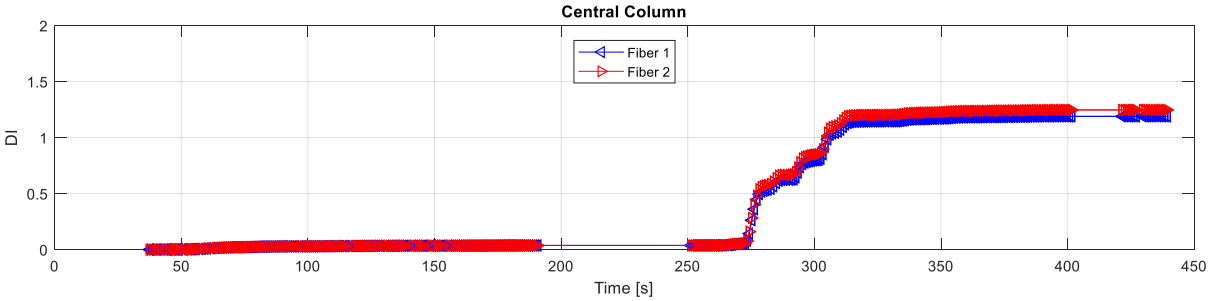

Fig. 9 – Damage index progression in time for both fibers of the central bottom column.

Although the SCT seismic record in the N90E generates the greatest demand among all records of the 1985 earthquake in terms of maximum inelastic displacement and dissipated hysteretic energy, it seems that no cyclic fatigue damage is generated during this period (Fig. 10). On the other hand, almost all damage is produced during 2017 seismic action where cumulative damage leads to a DI greater that 1 that means failure of reinforcing bars due to accumulation of fatigue plastic damage. Both fibers follow almost the same pattern as expected (symmetry). These results seem to be consistent with the damage observed in this type of structures after each earthquake (all damage concentrated in the 2017 earthquake). Even more, DI value matches with the fact that 4 structures of 5-6 stories height collapsed near SCT station in a radio of 1.5 km.

3.4 Low-Cycle Fatigue Damage Model Results

Same procedure is done for all records of the 2017 earthquake. For simplicity, DI associated to each seismic station is taken as the maximum of the N90E and N00E directions. Based on these results, a geostadistics processing of data called kriging is performed [22]. It is a powerful type of spatial interpolation formulation, anchored on the values at known points (stations). With this, contour lines of iso-DI can be constructed (Fig. 10). Yellow points represent the 4-7 story height collapsed buildings after 2017 earthquake, whose dynamic behavior could be similar to the prototype building considered in this study. Low-cycle fatigue damage model shows to have a good correlation with zone of damage concentration in Mexico City which is almost completely covered into iso-DI curve of value 0.8 (Fig. 10). Station SCT (in red) returns the highest DI while local soil effects can be noticed in the southern part of the map where there is also a yellow point.

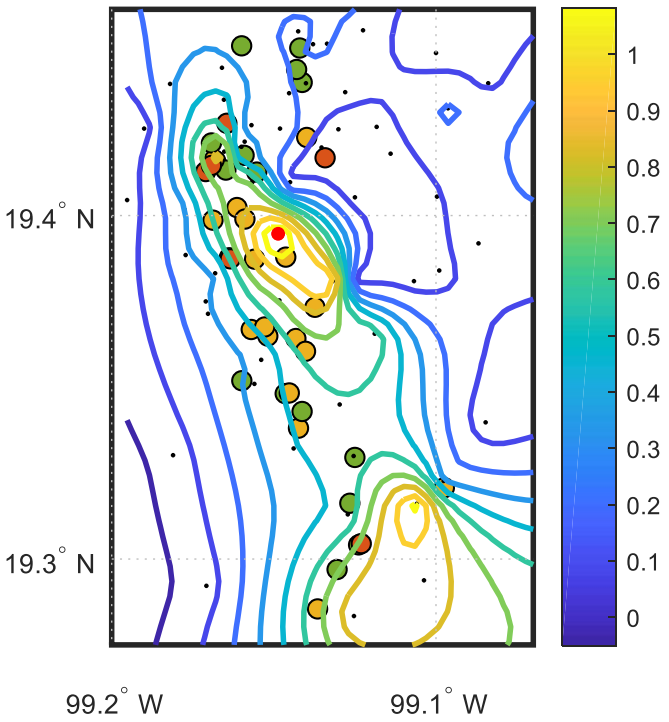

Fig. 10 – Iso-damage index curves considering low-cycle fatigue model.

3.4 SDOF Model Main Results

Maximum elastic/inelastic displacement (Sd) and hysteretic plastic energy (Eh) spectra is also calculated for all stations for the SDOF model. Firstly, iso-demand curves in terms of maximum displacement for a period T=1.5 seconds are plotted in Fig. 11. Taking in consideration that Fig. 10 concentrates the damage in the 2017 earthquake, Figs. 11 and 12 consider only the 2017 earthquake, even though some indices might increase with the addition of the 1985 earthquake.

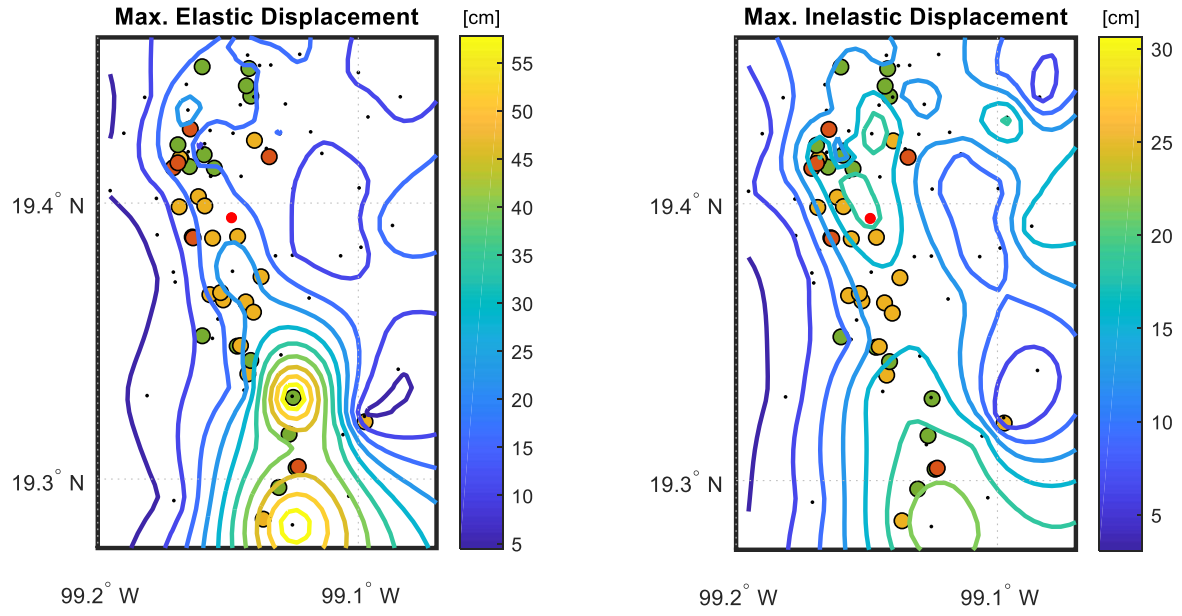

Fig. 11 – Iso-displacement curves for SDOF model: (a) elastic model, and (b) inelastic model.

Energy based damage index proposed and evaluated by Rodriguez [23] and by Park and Ang [1,24] are calculated from energy spectra. In the Rodriguez model, the parameter 'λ' , in s^{-1}, considers the structural resisting system and the soil below construction, which for the current prototype is assumed as an extremely flexible frame as defined by Rodriguez [5]. The second index damage combines a portion 'β' of dissipated energy and the ratio between maximum seismic ductility demand and ductility capacity (μ) of the system. According to maximum monotonic capacity of the prototype building with Q=2, a value of μ = 3.0 is defined [17]. When ductility demand reaches this value, collapse is expected. On the other hand, 'β' considers the impact of energy dissipation in damage. For RC structures, a value of β = 0.15 is proposed originally by Park *et al.* [1]. When β is high, the cumulative plastic damage becomes the cause of seismic failure. Typically, a high β value represents a poorly designed (and detailed) structure commonly available in old building stock [25]. In this study, the value of 0.25 is chosen. Finally, period of T=1.5 seconds is considered.

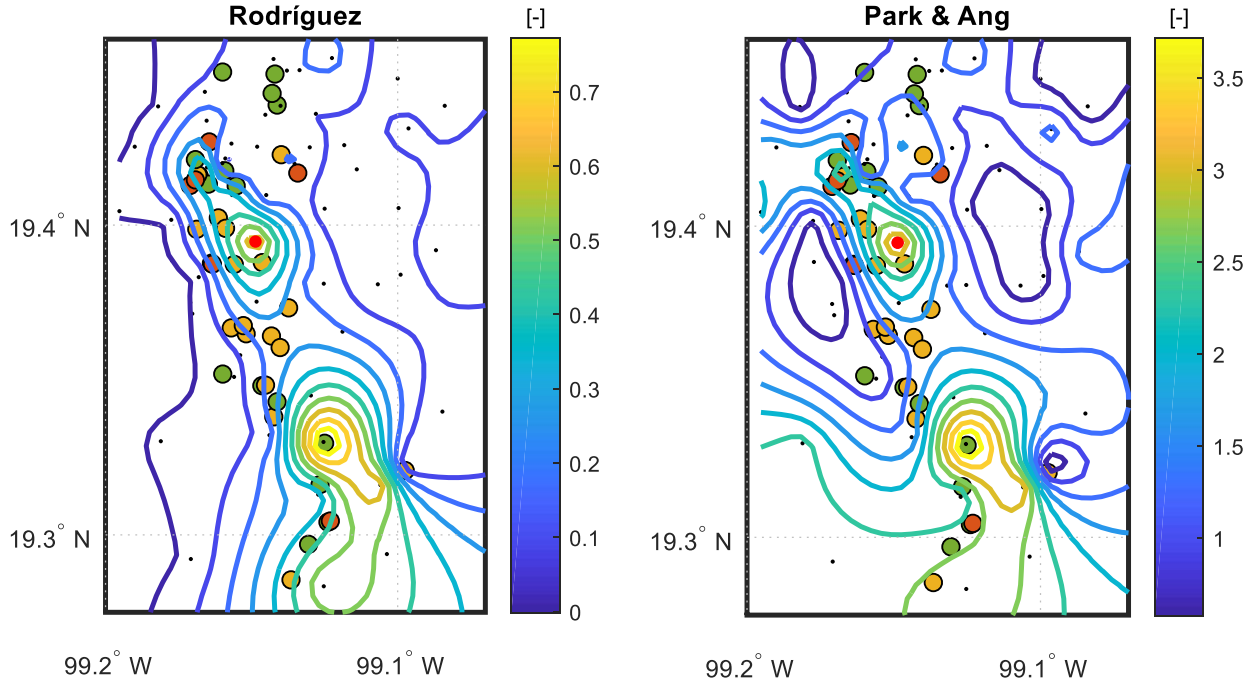

Fig. 12 – Iso-damage index for SDOF model. (a) Rodriguez, (b) Park and Ang.

Maximum displacement demands seem not to have the best concordance with yellow points (Fig. 11) as they consider only the maximum response of the system neglecting the number of cycles and cumulative damage. However, inelastic maximum displacement of 15-20 cm has the best match with the zone of damage. On the other hand, Rodriguez DI shows a good correlation with yellow dots (damage buildings) same as with Park and Ang DI. Simplified models cannot provide information regarding the distribution of damage within a structure as they are based on the first (single) mode response of the building [5], but comparison with maximum displacement graphs indicates that cumulative damage seems to be a more reasonable cause of the damage observed after the Puebla-Morelos 2017 earthquake.

5. Conclusions

In this work, the accumulated damage was studied through a fatigue damage model of the steel reinforcement in a representative prototype model of the structures mostly damaged after the Puebla-Morelos earthquake in 2017. Under certain considerations, the results of this damage index match the damage area quite well. This also happens with the accumulated damage for the simplified model that show a better correlation than the displacement spectra. This fact is quite concordant since the maximum displacement spectra are not as sensitive to the cyclic behavior of the structures as damage indexes, which played an important role in the

earthquake of 2017. Despite the accumulated damage results between the model of fatigue and the simplified model are quite similar, the first is much more realistic since it considers the response of a much more complex system and the local fatigue failure of the steel reinforcement of the first-floor columns. However, given the level of deformation of steel fibers, it is highly expected that this type of failure is accompanied by concrete crushing as it was seen in damaged buildings. Also, fatigue damage index values are based on a fatigue model of steel, so that, requires no calibration of a global damage index. It is also concluded that, for the model under consideration, the 1985 earthquake did not generate significant accumulation of damage on the structure prototype, which might not the case for all models.

5. Acknowledgements

The accelerograph records have been the product of the work of instrumentation and processing of the Seismic Instrumentation Unit of the Engineering Institute of the UNAM (RAII). The data used in this work were provided by the "Red Sísmica del Valle de México" (RSVM), belonging to the National Seismological Service [25]. Their valuable information is acknowledged.

6. References

[1] Park Y. J. and Ang A. H. S., Mechanistic seismic damage model for reinforced concrete, J. Struct. Eng. 111(4) (1985) 722–739.

[2] Cao VV, Ronagh HR, Ashraf M, Baji H. A new damage index for reinforced concrete structures. Earthquakes Struct 2014;6(6):581–609.

[3] Chai, Y. H. (2005). Incorporating low-cycle fatigue model into duration-dependent inelastic design spectra. *Earthquake Engineering and Structural Dynamics*, *34*(1), 83–96.

[4] Kunnath, S.K., Chai, Y.H. (2004). Cumulative damage-based inelastic cyclic demand spectrum. Earthquake Engineering and Structural Dynamics 33:4, 499-520.

[5] Rodriguez ME (2018): Damage index for different structural systems subjected to recorded earthquake ground motions. *Earthquake Spectra*, 34(2), 773–793.

[6] Teran-Gilmore, A., Bahena-Arredondo, N. (2008). Cumulative ductility spectra for seismic design of ductile structures subjected to long duration motions: Concept and theoretical background. *Journal of Earthquake Engineering*, *12*(1), 152–172.

[7] CICM. (2017). Preliminary summary of damages of the properties inspected by the brigades of the SICC of 09/19/2017 (in Spanish). Retrieved from Mexico City: https://docs.wixstatic.com/ugd/3e775b_6e4fff6862c749069396975e7c7f9a01.pdf

[8] Galvis, F., Miranda, E., Heresi, P., Dávalos, H., Silos, J. R. (2017). Preliminary Statistics of Collapsed Buildings in Mexico City in Puebla-Morelos Earthquake. (October), 17. Retrieved from http://www.learningfromearthquakes.org/2017-09-19-puebla-mexico/images/2017_09_19_Puebla_Mexico/pdfs/Preliminary_Report_Mexico2017_v7.pdf

[9] Mayoral, J. M., Hutchinson, T. C., Franke, K. W. (2017). Geotechnical engineering reconnaissance of the 19 September 2017 Mw 7.1 Puebla-Mexico City earthquake, GEER association report no. GEER-055A.

[10] Alberto, Y., Otsubo, M., Kyokawa, H., Kiyota, T., Towhata, I. (2018). Reconnaissance of the 2017 Puebla, Mexico earthquake. *Soils and Foundations*, *58*(5), 1073–1092.

[11] Hernández, F., Astroza, R., Ochoa, F., Pastén, C. (2019). Structural reasons for the collapse of buildings due to the Puebla-Morelos earthquake (Mw 7.1) (in Spanish). XII Congreso Chileno de Sismología e Ingeniería Sísmica, (1), 1–12.

[12] Gómez, A., Arellano, E., González, O., Juárez, H. (2017). Characteristics, causes, and consequences of the damages due to the earthquake of September 19, 2017 (M = 7.1) in Mexico 2017 (in Spanish). XII Congreso Chileno de Sismología e Ingeniería Sísmica, (1), 1–12.

[13] Roeslin, S., Ma, Q. T. M., & García, H. J. (2018). Damage Assessment on Buildings Following the 19th September 2017 Puebla, Mexico Earthquake. *Frontiers in Built Environment*, *4*(December), 1–18.

[14] Rodríguez, M. E. (2019). Conventional earthquake resistant design and accumulated damage. The case of damage and collapses in buildings in Mexico City in the earthquake of September 19, 2017 (in Spanish). XII Congreso Chileno de Sismología e Ingeniería Sísmica, (1), 1–12.

[15] Sismo 09/19/2017 CDMX Derrumbes. Retrieved from: https://www.google.com/maps/d/u/0/viewer?mid=18a98CKWjzoleGvBtOnbBVv5D4JA&ll=19.40354823345304%2C-99.13143420597697&z=14

[16] Google. (n.d.). Collapsed Building of Sataroga street, Mexico City. Retrieved July 20 2017.

[17] Arteta, C. A. *et al*. (2019). Response of Midrise Reinforced Concrete Frame Buildings to The 2017 Puebla Earthquake. *Earthquake Spectra*, 35(4),1–31.

[18] Newmark, N. M., Hall, W. J. (1982). Earthquake spectra and design. Monograph Series. Earthquake Engrg. Res. lnst., Berkeley, Calif.

[19] Tripathi, M., Dhakal, R. P., Dashti, F., & Massone, L. M. (2018). Low-cycle fatigue behaviour of reinforcing bars including the effect of inelastic buckling. *Construction and Building Materials*, *190*, 1226–1235.

[20] McKenna, F., Fenves, G. L., Scott, M. H., & Jeremic, B. (2000). Open system for earthquake engineering simulation (OpenSees) (Version 2.4.3.). Berkeley, CA: Pacific Earthquake Engineering Research Center, University of California.

[21] Downing, S. D., Socie, D. F. "Simple Rainflow Counting Algorithms", International Journal of Fatigue, V. 4, Issue 1, 1982, pp. 31 – 40.

[22] jBuist (2020). kriging(x,y,z,range,sill) (https://www.mathworks.com/matlabcentral/fileexchange/ 57133-kriging-x-y-z-range-sill), MATLAB Central File Exchange. Retrieved January 26, 2020.

[23] Rodriguez, M. E., and Aristizabal, J. C., 1999. Evaluation of a seismic damage parameter, Earthquake Engineering & Structural Dynamics 28, 463–477.

[24] Ghosh, S., Datta, D., & Katakdhond, A. A. (2011). Estimation of the Park-Ang damage index for planar multi-storey frames using equivalent single-degree systems. *Engineering Structures*, *33*(9), 2509–2524.

[25] Luis Quintanar, A. Cárdenas-Ramírez, D. I. Bello-Segura, V. H. Espíndola, J. A. Pérez-Santana, C. Cárdenas-Monroy, A. L. Carmona-Gallegos, I. Rodríguez-Rasilla (2018); A Seismic Network for the Valley of Mexico: Present Status and Perspectives; Seismological Research Letters, Volume 89, Number 2A, pp. 356-362, March/April 2018.

